REMUNOM
ISSN 2178-6925

Received: 13/01/2026 - **Accepted:** 02/04/2026
Vol: 13.05
DOI: 10.66104/qfmhys90
Pages: 1-33

ESTUDO DAS CONDIÇÕES DE PIRÓLISE DO RESÍDUO DE EXTRAÇÃO DE BURITI

STUDY OF THE PYROLYSIS CONDITIONS OF THE BURITI EXTRACTION RESIDUE

ESTUDIO DE LAS CONDICIONES DE PIRÓLISIS DEL RESIDUO DE EXTRACCIÓN DE BURITI

Natália de Diniz Martins
Master's student in Chemical Engineering, State University of Western Paraná (UNIOESTE), Toledo, Brazil
E-mail: nataliadinizmartins@gmail.com

Schaline Winck Alberti
Master's and PhD student in Chemical Engineering, State University of Western Paraná (UNIOESTE), Toledo, Brazil
E-mail: Schaline_swa@hotmail.com

Edson Antônio da Silva
PhD in Chemical Engineering, Professor at the State University of Western Paraná (UNIOESTE), Toledo, Brazil
E-mail: edsondeq@gmail.com

Plínio Ribeiro Fajardo Campos
PhD in Chemical Engineering, Professor at the State University of Western Paraná (UNIOESTE), Toledo, Brazil
E-mail: plinio.fajardo@hotmail.com

REMUNOM
ISSN 2178-6925

Received: 13/01/2026 - **Accepted:** 02/04/2026
Vol: 13.05
DOI: 10.66104/qfmhys90
Pages: 1-33

Resumo

Este estudo investigou a pirólise da biomassa de buriti visando a produção de biochar e bio-óleo sob diferentes condições operacionais. Os experimentos foram realizados em um reator de pirólise, variando temperaturas entre 450 °C e 600 °C e tempos de residência de 10 a 60 minutos. A análise termogravimétrica (TGA) revelou as diferentes etapas da degradação térmica da biomassa de buriti. O maior rendimento de biochar foi obtido a 450 °C por 30 minutos de pirólise (30,75%), enquanto o maior rendimento de bio-óleo foi alcançado a 525 °C por 60 minutos (48,98%). A análise de variância (ANOVA) demonstrou que a temperatura influenciou significativamente o rendimento de biochar, enquanto o tempo foi o principal fator para o aumento do rendimento de bio-óleo. O bio-óleo gerado apresentou poder calorífico superior (PCS) de 10,68 MJ kg^{-1}, enquanto o biochar apresentou um PCS significativamente maior de 30,664 MJ kg^{-1}. A análise espectroscópica por FTIR revelou a presença de grupos funcionais como fenóis, álcoois e compostos alifáticos. Os resultados demonstram que as condições operacionais influenciam diretamente a distribuição dos produtos, permitindo direcionar o processo para a obtenção de biochar ou bio-óleo.

Palavras-chave: Pirólise; Biochar; Bio-óleo; Biomassa de Buriti; Degradação Térmica e Rendimento.

Abstract

This study investigated the pyrolysis of buriti biomass aiming at the production of biochar and bio-oil under different operational conditions. Experiments were conducted in a pyrolysis reactor, varying temperatures between 450 °C and 600 °C and residence times from 10 to 60 minutes. Thermogravimetric analysis (TGA) revealed the distinct stages of buriti biomass thermal degradation. The highest biochar yield was obtained at 450 °C for 30 minutes of pyrolysis (30.75%), while the highest bio-oil yield was achieved at 525 °C for 60 minutes (48.98%). Analysis of variance (ANOVA) demonstrated that temperature significantly influenced biochar yield, while time was the main factor for increasing bio-oil yield. The generated bio-oil presented a higher heating value (HHV) of 10.68 MJ kg^{-1}, while the biochar showed a significantly higher HHV of 30.664 MJ kg^{-1}. FTIR spectroscopic analysis revealed the presence of functional groups such as phenols, alcohols, and aliphatic compounds. The results demonstrate that operational conditions directly influence product distribution, allowing the process to be directed towards obtaining either biochar or bio-oil.

Keywords: Pyrolysis; Biochar; Bio-oil; Buriti Biomass; Thermal Degradation and Yield.

Resumen

Este estudio investigó la pirólisis de la biomasa de buriti con el objetivo de producir biocarbón y bio-aceite bajo diferentes condiciones operacionales. Los experimentos se realizaron en un reactor de pirólisis, variando temperaturas entre 450 °C y 600 °C y tiempos de residencia de 10 a 60 minutos. El análisis termogravimétrico (TGA) reveló las diferentes etapas de la degradación térmica de la biomasa

REMUNOM
ISSN 2178-6925

Received: 13/01/2026 - **Accepted:** 02/04/2026
Vol: 13.05
DOI: 10.66104/qfmhys90
Pages: 1-33

de buriti. El mayor rendimiento de biocarbón se obtuvo a 450 °C durante 30 minutos de pirólisis (30,75%), mientras que el mayor rendimiento de bio-aceite se logró a 525 °C durante 60 minutos (48,98%). El análisis de varianza (ANOVA) demostró que la temperatura influyó significativamente en el rendimiento de biocarbón, mientras que el tiempo fue el factor principal para el aumento del rendimiento de bio-aceite. El bio-aceite generado presentó un poder calorífico superior (PCS) de 10,68 MJ kg^{-1}, mientras que el biocarbón mostró un PCS significativamente mayor de 30,664 MJ kg^{-1}. El análisis espectroscópico por FTIR reveló la presencia de grupos funcionales como fenoles, alcoholes y compuestos alifáticos. Los resultados demuestran que las condiciones operacionales influyen directamente en la distribución de los productos, permitiendo dirigir el proceso hacia la obtención de biocarbón o bio-aceite.

Palabras clave: Pirólisis; Biochar; Bio-aceite; Biomasa de Buriti; Degradación Térmica y Rendimiento.

1. Introduction

The necessity of seeking renewable fuel sources arises from the extensive use of fossil fuels, coupled with the inadequate management of solid waste, which presents significant challenges for the establishment of more sustainable systems. The pursuit of strategies to mitigate greenhouse gas emissions has adopted the valorization of biomass waste as a key approach, thereby developing and enhancing the conversion of these residues into value-added products and consequently reducing the emission of gases such as methane and carbon dioxide. (Gómez-Sanabria et al 2022).

In this context, bioenergy emerges as a promising alternative, as it relies on the conversion of renewable biomass into energy carriers with a lower carbon footprint. Biomass feedstocks typically contain lower concentrations of heteroatoms, particularly sulfur and nitrogen, compared to fossil fuels, which contributes to reduced pollutant emissions during conversion (Wang et al. 2022). Furthermore, the use of lignocellulosic residues reduces the demand for dedicated energy crops, promoting waste valorization.

Biomass is an abundant source of carbon, oxygen, hydrogen, and nitrogen that can be converted and reused. Its lignocellulosic fraction can be converted by thermal processes in an inert atmosphere through pyrolysis, in which the decomposition of biomass promotes the formation of three main co-products: biochar, bio-oil, and

REMUNOM
ISSN 2178-6925

Received: 13/01/2026 - **Accepted:** 02/04/2026
Vol: 13.05
DOI: 10.66104/qfmhys90
Pages: 1-33

syngas (non-condensable gases), whose distribution depends on operational conditions, especially temperature and residence time (Amenaghawon et al 2021; Aboelela et al 2023). Hemicellulose and cellulose decompose at lower temperatures, producing volatile compounds that lead to condensable liquids and non-condensable gases. In contrast, lignin exhibits higher thermal stability and contributes significantly to biochar formation. Higher temperatures promote secondary reactions, such as thermal cracking, thereby enhancing gas yield, whereas lower temperatures favor biochar production (Jerzak et al 2024).

Among biomass resources with energy potential in Brazil, the buriti palm (*Mauritia flexuosa*) stands out due to its wide distribution in the Amazon and Cerrado regions. The processing of its fruits, directed toward the food and cosmetic industries, generates significant amounts of lignocellulosic residues that are still underutilized. These residues exhibit favorable characteristics for energy applications, including low ash content, high calorific value, and high lignin content (Silva et al 2023).

To systematically evaluate the influence of these variables, statistical tools such as the Central Composite Rotational Design (CCRD) and Response Surface Methodology (RSM) are widely employed, allowing for the analysis of individual and interaction effects among process factors (Aboelela et al 2023; Myers et al 2016).

Despite advances in this field, gaps remain regarding the utilization of buriti waste (lignocellulosic cake) under different pyrolysis conditions. In this context, this study aims to evaluate the effects of temperature and residence time on the production of biochar and bio-oil from this residue using an experimental design approach, with emphasis on identifying product distribution patterns within the investigated range.

2. Methodology

2.1 Raw material and preparation

The buriti (Mauritia flexuosa) residue used in this study corresponds to the solid fraction remaining after oil extraction from the fruit pulp, characterized as a lignocellulosic cake resulting from agro-industrial processing. After this stage, the material was subjected to natural drying in an open environment until constant mass was achieved, with the moisture content determined by proximate analysis (Section

REMUNOM
ISSN 2178-6925

Received: 13/01/2026 - **Accepted:** 02/04/2026
Vol: 13.05
DOI: 10.66104/qfmhys90
Pages: 1-33

2.3). The samples were used without additional pre-treatments, such as grinding or particle size classification, being employed directly as received. For each experiment, approximately 30 g of biomass were used, and the samples were stored under ambient conditions until the tests were performed.

The choice of this residue as a raw material is associated with its availability and the potential for valorization of by-products from the buriti agro-industrial chain. It is noteworthy that the use of the residual cake, in its unprocessed form, seeks to represent real conditions for the utilization of these residues. However, the lack of standardization regarding particle size and material composition constitutes an experimental limitation, which may influence the reproducibility and variability of the results obtained.

2.2 Thermogravimetric Analysis (TGA)

Thermogravimetric analysis was conducted with the aim of characterizing the thermal degradation stages of the lignocellulosic cake, contributing to the definition of the temperature range adopted in the experimental design. The sample was analyzed using a TG-DTG equipment (PerkinElmer, STA 600). Approximately 10 mg of each sample were placed in a porcelain sample holder and subjected to heating from 30 °C to 900 °C under an inert nitrogen (N_2) atmosphere. The heating rate employed was 10 °C min^{-1}, with a carrier gas flow of 20 mL min^{-1}.

2.3 Immediate Analysis By TGA

The proximate composition of the samples was determined by thermogravimetric analysis, based on the methodology adapted from Saldarriaga et al. (2015), allowing the quantification of moisture, volatile matter, fixed carbon, and ash contents.

The sample was subjected to programmed heating in a TG-DTG equipment (PerkinElmer, STA 600). Initially, the samples were heated from 30 °C to 105 °C under a nitrogen (N_2) atmosphere, at a heating rate of 15 °C min^{-1} and a gas flow of 60 mL min^{-1}, followed by an isothermal step of 80 minutes at this temperature. In the

REMUNOM
ISSN 2178-6925

Received: 13/01/2026 - **Accepted:** 02/04/2026
Vol: 13.05
DOI: 10.66104/qfmhys90
Pages: 1-33

subsequent stage, the temperature increased to 700 °C, maintaining the same operating conditions, with the application of a 30-minute isothermal period for the determination of the volatile matter fraction. Subsequently, the carrier gas was replaced with synthetic air, while maintaining the temperature at 700 °C for 5 minutes, a step intended for the quantification of ash content. At the end of the test, the system was cooled down to 30 °C. A detailed description of the procedure can be observed in Figure 1 (adapted from Saldarriaga et al 2015).

Figure 1 - Methodology developed for immediate analysis by TGA.

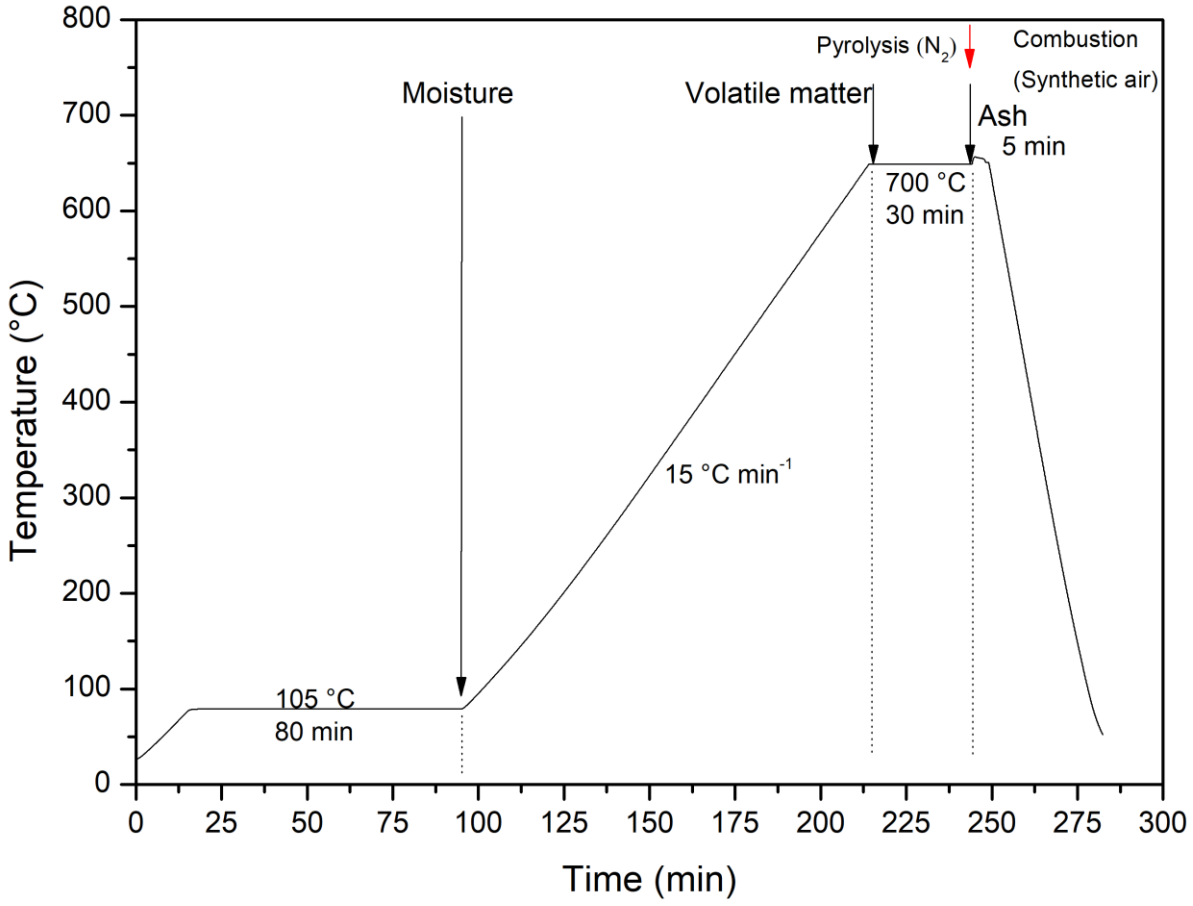

Source: Adapted from Saldarriaga *et al*. (2015).

2.4 Rotational Central Composite Design (CCRD)

The experimental study was conducted based on a Central Composite Rotatable Design (CCRD), with the aim of evaluating the influence of operational variables on the yields of pyrolysis products. As independent variables, reaction

REMUNOM
ISSN 2178-6925

Received: 13/01/2026 - **Accepted:** 02/04/2026
Vol: 13.05
DOI: 10.66104/qfmhys90
Pages: 1-33

temperature (°C), and residence time (min) were considered. The experimental design was structured based on a 2^2 factorial arrangement, with the addition of four axial points (±1.41) and four replicates at the central point, totaling 12 experiments. The response variables analyzed corresponded to the yields of biochar (y_1) and bio-oil (y_2), both expressed as percentages.

Data analysis was performed using Statistica software, adopting a significance level of 95% ($p < 0.05$). Linear, quadratic, and interaction effects between the variables were investigated, in addition to the fitting of empirical models using response surface methodology.

Table 1 - Experimental conditions of the design.

Variable	**-1.41**	**-1**	**0**	**1**	**+1.41**	**Code**
Temperature (°C)	450	472	525	578	600	**x1**
Pyrolysis Isotherm (min)	10	16	30	51	60	**x2**

Source: Prepared by the authors.

Table 2 presents the CCRD experimental design matrix, in which the conditions applied in each run are described, expressed in terms of coded variables.

Table 2. CCRD design matrix.

Run	**x1**	**x2**
1	-1	-1
2	1	-1
3	-1	1
4	1	1
5	-1.41	0
6	1.41	0
7	0	-1.41
8	0	1.41
9	0	0
10	0	0
11	0	0
12	0	0

Source: Prepared by the authors.

REMUNOM
ISSN 2178-6925

Received: 13/01/2026 - **Accepted:** 02/04/2026
Vol: 13.05
DOI: 10.66104/qfmhys90
Pages: 1-33

2.5 Biochar and Bio-oil Production

The pyrolysis experiments were conducted in a fixed-bed reactor under an inert nitrogen (N_2) atmosphere, with a constant flow rate of 100 mL min^{-1}. The samples were heated at an approximate rate of 20 °C min^{-1} up to the temperature defined in the experimental design. Once this value was reached, the system was maintained under isothermal conditions for the time corresponding to each run.

The vapors generated during the process were directed at a condensation system, allowing the collection of liquid fractions (bio-oil), while the biochar remained inside the reactor at the end of the operation.

2.6 Yield

The evaluation of yield (y_1) consists of determining the ratio between the mass of the carbonized product (m_{prod}), obtained after pyrolysis, and the mass of the raw biomass (m_{biom}). Similarly, the bio-oil yield (y_2) is determined by the ratio between the mass of the bio-oil produced (m_{prod}) and the mass of the raw biomass (m_{biom}). The yields are expressed as percentages and reflect the fraction of the original mass converted into bio-oil and biochar during the pyrolysis process. The calculation follows Equation 1.

$$y(\%) = \frac{m_{prod}}{m_{biom}} * 100 \quad (1)$$

2.7 Characterization of Co-products

2.7.1. Higher Heating Value

The higher heating value of the samples was determined using a bomb calorimeter. For this purpose, approximately 0.3 g of each sample were weighed and placed into crucibles.

Subsequently, the material was connected to the ignition system by means of a cotton thread and subjected to combustion in an oxygen atmosphere under a pressure of approximately 30 atm. Finally, the sample was placed in the calorimetric bomb for the determination of the heating value.

REMUNOM
ISSN 2178-6925

Received: 13/01/2026 - **Accepted:** 02/04/2026
Vol: 13.05
DOI: 10.66104/qfmhys90
Pages: 1-33

2.7.2. Fourier Transform Infrared Spectroscopy (FTIR)

The identification of functional groups present in the biochar and bio-oil was conducted by infrared absorption spectroscopy, both before and after the adsorption process. The samples were prepared by dispersion in potassium bromide (KBr) until the formation of a thin film. The analysis was conducted using a Fourier transform infrared (FTIR) spectrophotometer, operating in the range of 4000 to 400 cm^{-1}, with a resolution of 4.0 cm^{-1}.

3. RESULTS AND DISCUSSION

3.1 Thermogravimetric Analysis (TGA)

Thermogravimetric analysis (TGA) allows you to monitor the mass variation of a material as a function of temperature, being an important tool to identify the stages of thermal decomposition of biomass. In the evaluated material (Figure 2), the range between 30 and 150 °C corresponds to the removal of moisture and lighter compounds, corresponding to approximately 10% of the initial mass. While between 200 and 400 °C, there is a loss of 45% of the mass, which is related to the decomposition of the main more reactive lignocellulosic constituents (hemicellulose and cellulose), which is associated with the release of volatile compounds from the biomass. Being consistent with the decomposition of hemicellulose and cellulose, which are concentrated in this temperature range.

REMUNOM
ISSN 2178-6925

Received: 13/01/2026 - **Accepted:** 02/04/2026
Vol: 13.05
DOI: 10.66104/qfmhys90
Pages: 1-33

Figure 2 - Thermogravimetric analysis of Buriti.

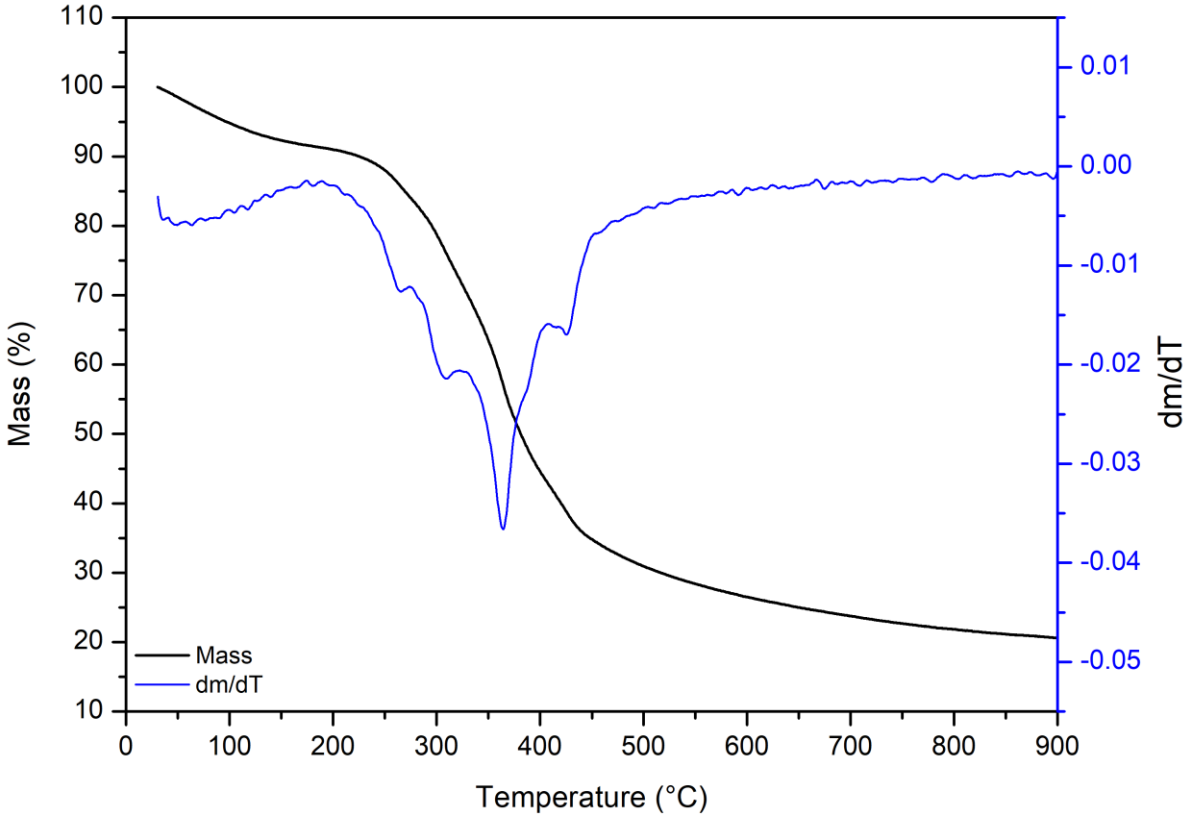

Source: Prepared by the authors.

At temperatures above 500 °C, they are related to the degradation of more condensed and thermally stable structures, such as lignin, which presents more gradual degradation and is responsible for the higher yield and formation of char. Its degradation is distributed over a wider range and can extend to about 800 °C (Consumi et al 2022; Sousa et al 2024).

Based on these results, the temperature range between 450 °C and 600 °C was defined for the experimental design, to cover the region of greatest thermal degradation of the volatiles and favor the formation of biochar and bio-oil.

3.2 Immediate Analysis By TGA

The proximate analysis obtained by TGA provides relevant information about the composition of the material, including the contents of moisture, volatile matter, ash, and fixed carbon. The results are presented in Table 3 on a wet basis.

REMUNOM
ISSN 2178-6925

Received: 13/01/2026 - **Accepted:** 02/04/2026
Vol: 13.05
DOI: 10.66104/qfmhys90
Pages: 1-33

The moisture content of 7.69% indicates that the material presents a low amount of residual water, which is favorable from an energy standpoint, as it reduces the heat demand required for evaporation during heating, thereby contributing to the efficiency of the pyrolysis process. Ferreira et al. (2021) obtained a moisture content of 8.3% for lignocellulosic cake, while Silva et al. (2023) reported moisture values between 11.27 and 12.82% for peels and seeds, thus highlighting differences between materials previously subjected to pulp and oil extraction.

Table 3. Proximate analysis of lignocellulosic cake residue from buriti pulp/oil extraction, compared with data reported in the literature.

Component	Moisture (%)	Volatile matter (%)	Ash (%)	Fixed carbon (%)	References
Lignocellulosic buriti cake	7.69	74.70	3.36	14.25	Author
Buriti pit (%)	12.82	84.67	3.17	3.34	Silva et al (2023)
Buriti bark (%)	11.27	68.47	2.60	17.66	Silva et al (2023)
Buriti cake (%)	8.3	--	5.2	--	Ferreira et al (2021)
Endocarp	8.81	85.00	4.66	10.34	Guimarães et al (2021)

Source: Prepared by the authors.

Volatile matter was the predominant fraction, with 74.70%, indicating high thermal reactivity of the material, being associated with a greater release of volatile and condensable compounds during heating, favoring the formation of bio-oil and non-condensable gases (syngas). When compared to different parts of buriti, the volatile matter content ranges from 85% for the endocarp to 68.47% for the peel. (Guimarães et al 2021, Silva et al. 2023)

The ash content of 3.36% can be considered low, indicating a reduced presence of inorganic material. This characteristic is relevant, as high ash contents may compromise process efficiency, in addition to promoting operational problems, such as deposit formation and interference in thermal reactions. The fixed carbon content, corresponding to 14.25%, is related to the solid fraction remaining after the release of volatiles, contributing to char formation and to the energy content of the material. This parameter is also associated with the thermal stability of the residue

REMUNOM
ISSN 2178-6925

Received: 13/01/2026 - **Accepted:** 02/04/2026
Vol: 13.05
DOI: 10.66104/qfmhys90
Pages: 1-33

and its potential for energy utilization. Silva et al. (2023) reported 17.66% for buriti peel, while Guimarães et al. (2021) reported 10.34% for the endocarp of the fruit.

The values obtained are consistent with those commonly reported for lignocellulosic biomasses, which typically present a high volatile matter fraction and low moisture and ash contents, favoring thermal degradation and performance in thermochemical conversion processes (Racero-Galaraga et al. 2024). In addition, the observed relationship between volatile matter and fixed carbon indicates an adequate balance between the formation of condensable products and the generation of the solid fraction, as discussed in kinetic studies of thermal degradation (Emiola-Sadiq et al. 2021).

Therefore, the results confirm that buriti residue presents properties compatible with its use in thermochemical processes, highlighting its high volatile matter content, low mineral fraction, and suitable moisture content.

3.3 Yield

Based on the experimental yields of biochar and bio-oil obtained from the pyrolysis experiments (Table 4), the overall mass balance of the process was determined in terms of yield (%), considering the distribution of products into three main fractions: solid (biochar), liquid (bio-oil), and gaseous (non-condensable gases). The gaseous fraction was not directly quantified in this study and was therefore estimated by difference, which represents a limitation of the study, as it does not allow the determination of its composition nor the direct quantification of possible experimental losses, such as incomplete condensation or leaks. Thus, the obtained values should be interpreted as estimates of the overall mass distribution.

Biochar yields were obtained in the range of 27–31%, bio-oil yields between 31–49%, and syngas yields between 25–40%. It was observed that the highest biochar yield was obtained in run 5 (30.75%), corresponding to the condition of 450 °C and 30 minutes. This result indicates that lower temperatures favor the formation of the solid fraction, as they limit the occurrence of secondary reactions, promoting greater carbon retention in the material.

REMUNOM
ISSN 2178-6925

Received: 13/01/2026 - **Accepted:** 02/04/2026
Vol: 13.05
DOI: 10.66104/qfmhys90
Pages: 1-33

Table 4 - Yields of co-products obtained from the pyrolysis of buriti residue.

Run	Biochar (%)	Bio-oil (%)	Syngas (%)
1	29.23	31.11	39.66
2	27.71	42.63	29.66
3	29.67	41.91	28.42
4	27.51	41.11	31.38
5	30.75	38.41	30.84
6	27.14	45.80	27.06
7	29.34	34.49	36.17
8	28.14	48.98	22.88
9	28.19	44.62	27.19
10	28.63	45.91	25.46
11	28.41	41.08	30.51
12	28.10	43.72	28.18

Source: Prepared by the authors.

In contrast, the highest bio-oil yield was recorded in run 8 (48.98%), under the conditions of 525 °C and 60 minutes. This indicates that intermediate temperatures, combined with longer residence times, favor the formation and recovery of condensable compounds. In general, a transition in the product distribution profile is observed: milder conditions favor biochar formation, while increasing operational severity shifts the distribution toward the liquid fraction.

The gaseous fraction ranged from 22.88% to 39.66%, reflecting the influence of operational conditions on product distribution, reaching its maximum yield in run 1 (450 °C and 10 min). In general terms, configurations that maximize bio-oil production tend to reduce gas formation, while increasing temperature and/or intensifying thermal exposure time favor secondary reactions, such as vapor cracking, resulting in greater generation of non-condensable gases.

The different yield values can be explained by the progressive conversion of lignocellulosic fractions, which, under more severe conditions, are distributed differently. During pyrolysis, the degradation of structural constituents (cellulose, hemicellulose, and lignin) leads to the formation of volatile intermediates that can be

REMUNOM
ISSN 2178-6925

Received: 13/01/2026 - **Accepted:** 02/04/2026
Vol: 13.05
DOI: 10.66104/qfmhys90
Pages: 1-33

condensed as bio-oil or converted into gases through secondary reactions, such as cracking and reforming (Emiola-Sadiq et al 2021; Wang et al. 2020).

Emiola-Sadiq et al. (2021) evaluated the formation of biochar and volatiles (condensable and non-condensable) for lignocellulosic biomasses under different heating rates through thermogravimetric analysis, obtaining yields like those obtained for buriti residue. Biochar yields of 29.1% (soybean hull), 23.1% (oat husk), 6.8% (fir), and 20% (willow) were obtained, while volatile yields were 70.9% (soybean hull), 76.9% (oat husk), 93.2% (fir), and 80% (willow) at a heating rate of 20 °C min^{-1}, similar to that employed in the experimental design.

3.4 Analysis of Variance (ANOVA)

The evaluation of biochar and bio-oil yields was carried out based on the experimental data presented in Table 4 and subsequently subjected to analysis of variance (ANOVA), whose results are presented in Tables 5 and 6. The residual analysis (Appendix I – Figures A and B) showed a random distribution of points, without a defined trend, indicating the absence of evident inconsistencies in the model conditions. In the observed versus predicted value plots (Appendix I – Figures C and D), the proximity of the points to the identity line reinforces the predictive capacity of the fitted models.

For the ANOVA of biochar yield (Table 5), the fitted model presented a coefficient of determination $R^2 = 0.905$ and an adjusted $R^2 = 0.826$, indicating that approximately 82.6% of the variability in the data is explained by the model within the investigated experimental range. Temperature exhibited a highly significant linear effect (p- value = 0.001), highlighting its role as the main variable controlling biochar formation. In contrast, residence time (p-value = 0.12), the quadratic terms (p-value > 0.05), and the interaction between temperature and time (p-value = 0.27) did not show statistical significance at the 95% confidence level.

The data analysis demonstrates that, under the evaluated conditions, biochar yield is governed by temperature, with an approximately linear behavior. The lack of significance of the quadratic terms suggests that there is no consistent evidence of curvature in the response surface for this product. This agrees with studies that

REMUNOM
ISSN 2178-6925

Received: 13/01/2026 - **Accepted:** 02/04/2026
Vol: 13.05
DOI: 10.66104/qfmhys90
Pages: 1-33

investigated the pyrolysis of lignocellulosic biomasses, in which increasing temperature promotes the intensification of devolatilization reactions, reducing biochar yield. Equivalent results have been reported for different agro-industrial residues, indicating that the solid fraction tends to decrease under more severe process temperatures. Thus, establishing an inverse relationship between temperature and biochar yield (Silva et al 2023; Emiola-Sadig et al 2021).

Table 5. ANOVA for Biochar Yield

	SQ	GL	MQ	F	p-Value
(1) Temperature (°C) (L)	9.63	1.00	9.63	170.38	0.001
Temperature (°C) (Q)	0.34	1.00	0.34	5.95	0.09
(2) Time (min) (L)	0.26	1.00	0.26	4.65	0.12
Time (min) (Q)	0.10	1.00	0.10	1.77	0.28
Temp. X time (L)	0.10	1.00	0.10	1.78	0.27
Model	10.37	5.00	2.07	11.44	0.01
Lack of fit	0.92	3.00	0.31	5.42	0.10
Pure error	0.17	3.00	0.06		
Residual	1.09	6.00	0.18		
Total	11.46	11.00			

R^2 = 0.90504; R^2 Adj = 0.82591; Pure error = 0.0565061.

Source: Prepared by the authors.

The lack-of-fit analysis (p-value = 0.10) indicates that, although the model is significant, its predictive capability presents limitations. This suggests that factors not considered, such as variations in the effective heating rate, heat transfer, or biomass heterogeneity, may influence the results. Due to these limitations, it was decided not to present the fitted predictive equations, as the model did not exhibit sufficient robustness. Future studies with a greater number of experiments and refinement of the experimental range may contribute to improved model robustness.

For bio-oil yield (Table 6), the model presented R^2= 0.844 and an adjusted R^2=0.714, indicating a moderate fit to the experimental data. Unlike what was observed for biochar, both temperature (p-value = 0.035) and residence time (p-value

REMUNOM
ISSN 2178-6925

Received: 13/01/2026 - **Accepted:** 02/04/2026
Vol: 13.05
DOI: 10.66104/qfmhys90
Pages: 1-33

= 0.014) showed significant linear effects, highlighting the combined influence of these variables on bio-oil formation.

The interaction term temperature vs. time presented a p-value = 0.057, a value close to the significance threshold. This suggests an interaction trend between the variables, although it cannot be statistically confirmed at the 95% confidence level. Thus, any interpretation in this regard should be made with caution. The quadratic terms were not significant (p-value > 0.05), indicating the absence of robust statistical evidence of nonlinear behavior within the studied range. The lack-of-fit analysis (p-value = 0.24), in turn, suggests that the model is adequate to describe the experimental data, within the limitations of the adopted design.

Table 6. ANOVA for Bio-oil Yield.

	SQ	GL	MQ	F	p-Value
(1) Temperature (°C) (L)	55.98	1	55.98	13.39	0.035
Temperature (°C) (Q)	15.34	1	15.34	3.67	0.151
(2) Time(min) (L)	110.71	1	110.71	26.49	0.014
Time (min) (Q)	19.25	1	19.25	4.61	0.121
Temp. X time (L)	37.95	1	37.95	9.08	0.057
Model	233.58	5	46.72	6.50	0.020
Lack of fit	30.56	3	10.19	2.44	0.241
Pure error	12.54	3	4.18		
Residual	43.10	6	7.18		
Total	276.69	11			

R^2 = 0.84422; R^2 Adj = 0.7144, Pure error = 4.179034.

Source: Prepared by the authors.

Some studies report that bio-oil yield is maximized at intermediate temperatures, due to the balance between the formation of volatile compounds and their secondary degradation. At higher temperatures, studies indicate that reactions such as thermal cracking and thermal reforming become predominant, reducing the liquid fraction and increasing gas formation. Thus, the maximum bio-oil yield observed at 525 °C and 60 min can be attributed to this balance between the generation and degradation of volatiles. At 600 °C, the increase in reaction severity intensifies the conversion of

REMUNOM
ISSN 2178-6925

Received: 13/01/2026 - **Accepted:** 02/04/2026
Vol: 13.05
DOI: 10.66104/qfmhys90
Pages: 1-33

liquid compounds into gaseous fractions, justifying the reduction in bio-oil yield (Wang et al. 2020).

Residence time also plays a relevant role in this process. Longer times favored biomass conversion and the release of volatiles; however, depending on the thermal conditions, they may intensify secondary degradation reactions of bio-oil. In the present study, the results indicate that increasing residence time still contributes positively to the yield, suggesting that the operating regime has not yet reached an optimum point at which these reactions become predominant (Emiola-Sadiq et al 2021; Aboelela et al 2023).

The Pareto diagram for biochar yield (Figure 3) illustrates the magnitude and statistical significance of the standardized effects of the experimental factors. In the graph, the red line represents the critical value for p = 0.05, such that the bars that exceed it indicate significant effects at the 5% level.

Figure 3 - Pareto diagram for biochar yield.

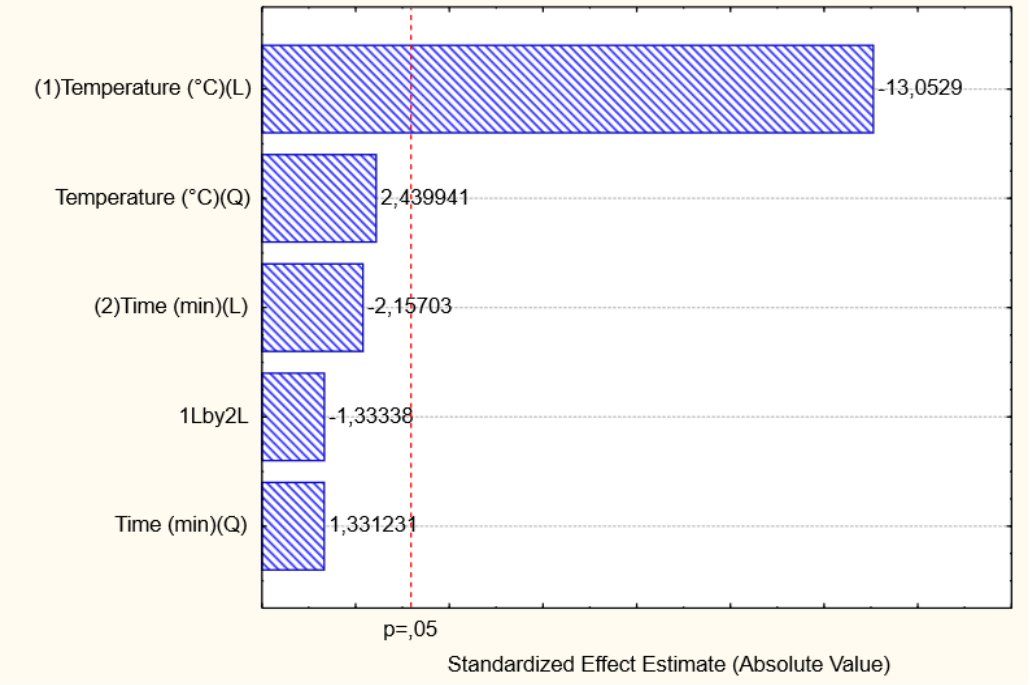

Source: Prepared by the authors.

It was observed that temperature (°C) is the most influential variable on biochar yield, in agreement with the ANOVA results, presenting a standardized effect higher

REMUNOM
ISSN 2178-6925

Received: 13/01/2026 - **Accepted:** 02/04/2026
Vol: 13.05
DOI: 10.66104/qfmhys90
Pages: 1-33

than the other factors and above the significance threshold. This result reinforces that biochar yield is strongly associated with temperature, highlighting the importance of controlling this parameter for process optimization.

The Pareto diagram for bio-oil yield (Figure 4) reveals a distinct influence pattern. In this case, residence time stands out as the most significant factor, followed by temperature, both exceeding the critical value for p-value = 0.05. These results indicate that bio-oil yield is influenced by residence time and, to a lesser extent, by temperature.

Figure 4 - Pareto diagram for bio-oil yield.

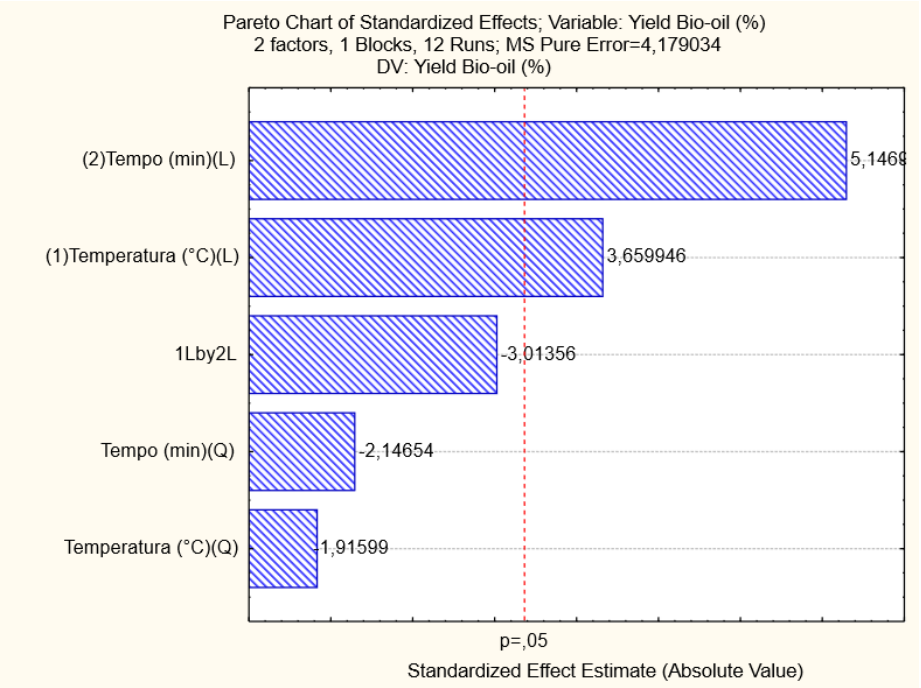

Source: Prepared by the authors.

Finally, the analysis of response surfaces is an important step for interpreting system performance as a function of the investigated operational variables. Figures 5 and 6 present, respectively, the three-dimensional (3D) and two-dimensional (2D) surfaces for biochar yield. From Figure 5, it was observed that temperature exerts a predominant influence on biochar yield, which is reflected in the steeper slope of the surface along this axis. With increasing temperature, there is a significant reduction in yield, in which warmer tones represent higher yields and cooler tones represent

REMUNOM
ISSN 2178-6925

Received: 13/01/2026 - **Accepted:** 02/04/2026
Vol: 13.05
DOI: 10.66104/qfmhys90
Pages: 1-33

lower yields. This behavior is related to the intensification of devolatilization and thermal cracking reactions at higher temperatures, which favor the formation of liquid and gaseous fractions at the expense of the solid carbonaceous fraction.

Figure 6 (2D surface) confirms this linear profile, highlighting the effect of temperature on biochar yield, in agreement with the results of the analysis of variance (Table 5), in which only the linear term of temperature showed statistical significance. On the other hand, residence time exhibited a less pronounced influence, reflected in the low curvature of the surface along this axis. This indicates that, within the evaluated experimental range, time does not function as a limiting factor in biochar formation, and the process is controlled by temperature. This result is also consistent with the thermal effect observed in the thermogravimetric analysis (Figure 2), in which the main biomass degradation occurs within specific temperature ranges.

Figure 5 - Graph of the 3D response surface for biochar.

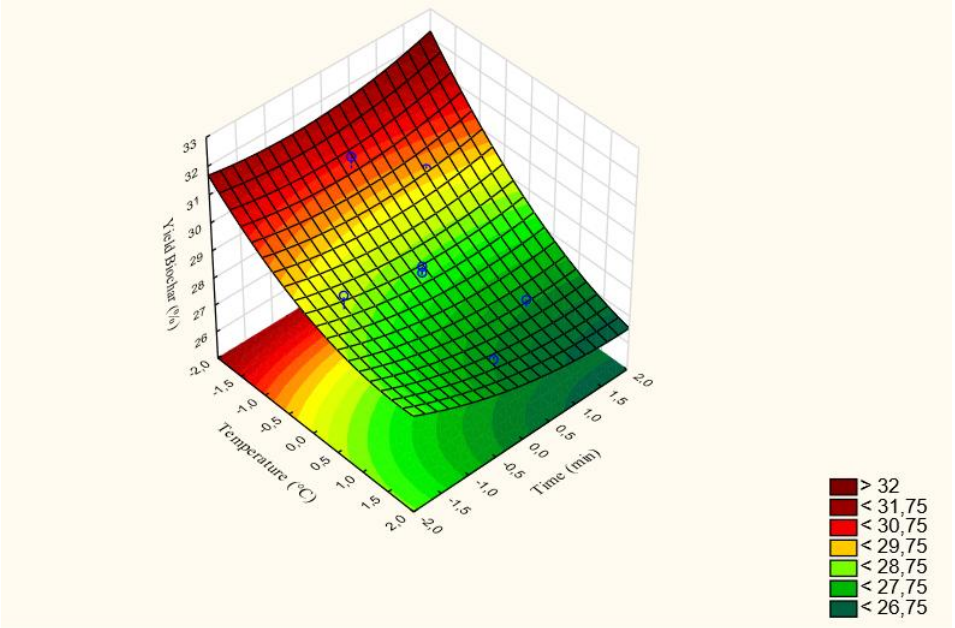

Source: Prepared by the authors.

REMUNOM
ISSN 2178-6925

Received: 13/01/2026 - **Accepted:** 02/04/2026
Vol: 13.05
DOI: 10.66104/qfmhys90
Pages: 1-33

Figure 6 - Graph of the 2D response surface for biochar.

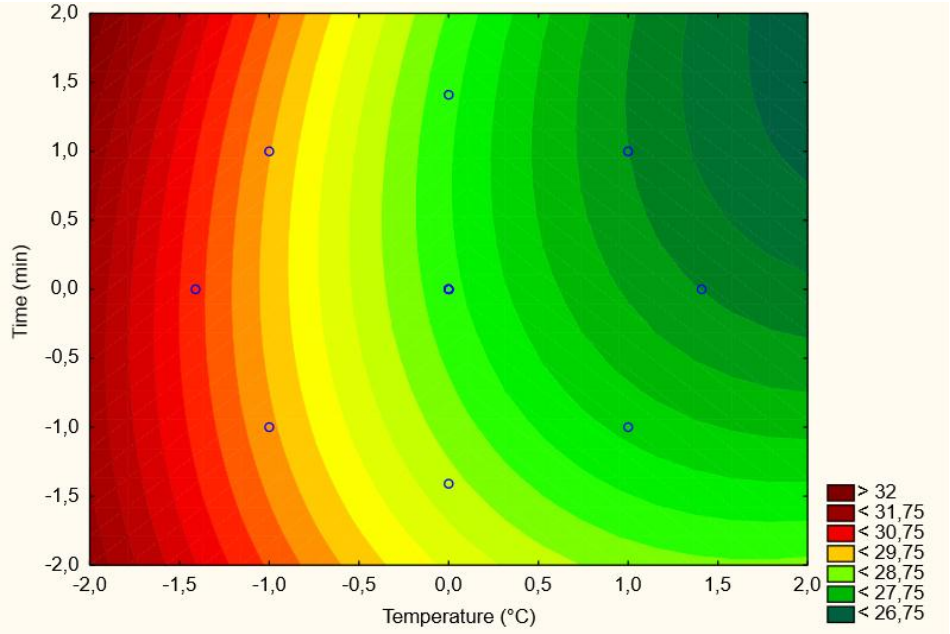

Source: Prepared by the authors.

In contrast, Figures 7 and 8 present the response surfaces for bio-oil yield, showing a distinct profile compared to biochar. It was observed that both temperature and residence time exert a positive influence on bio-oil yield, with this effect being more pronounced when both variables increase simultaneously. The surface exhibits a maximum region near the central point of the experimental design (approximately 525 °C and 60 minutes), in which the critical values estimated by the model indicate a maximum at a coded temperature of −1.67 and a time of 2.55. However, it was observed that the critical time value lies outside the experimental range studied, indicating that the optimal condition was not fully achieved within the investigated domain.

Based on these results, it is suggested that the maximization of bio-oil yield is associated with the combination of intermediate temperatures and longer residence times. For future studies, it is recommended to expand the residence time range (for example, up to 120 minutes), especially in regions close to the identified optimal temperature.

REMUNOM
ISSN 2178-6925

Received: 13/01/2026 - **Accepted:** 02/04/2026
Vol: 13.05
DOI: 10.66104/qfmhys90
Pages: 1-33

Figure 7 - Graph of the 3D response surface for the bio-oil.

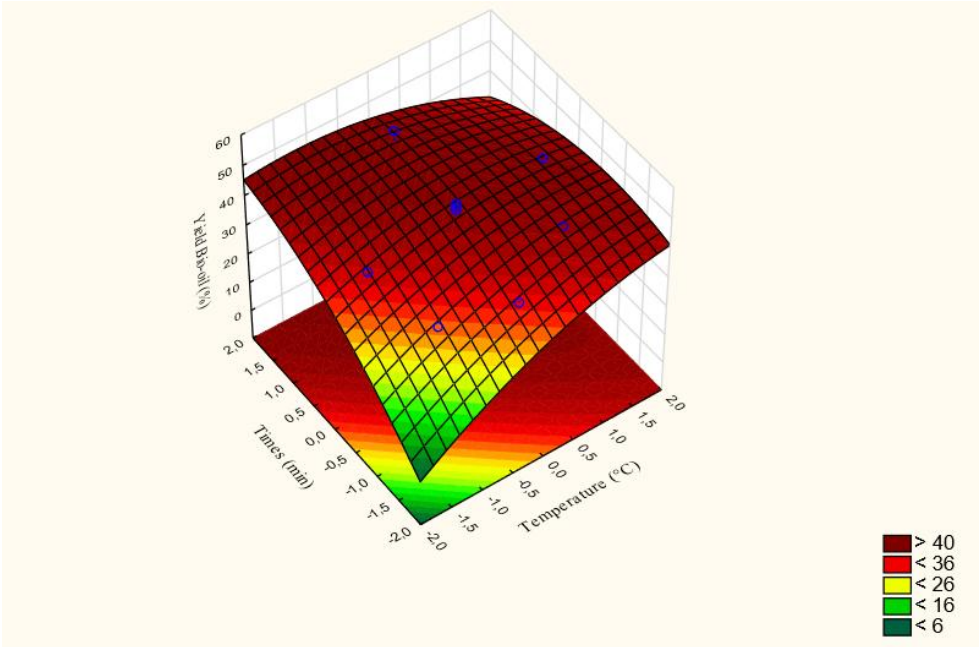

Source: Prepared by the authors.

Figure 8 - Graph of the 2D response surface for the bio-oil.

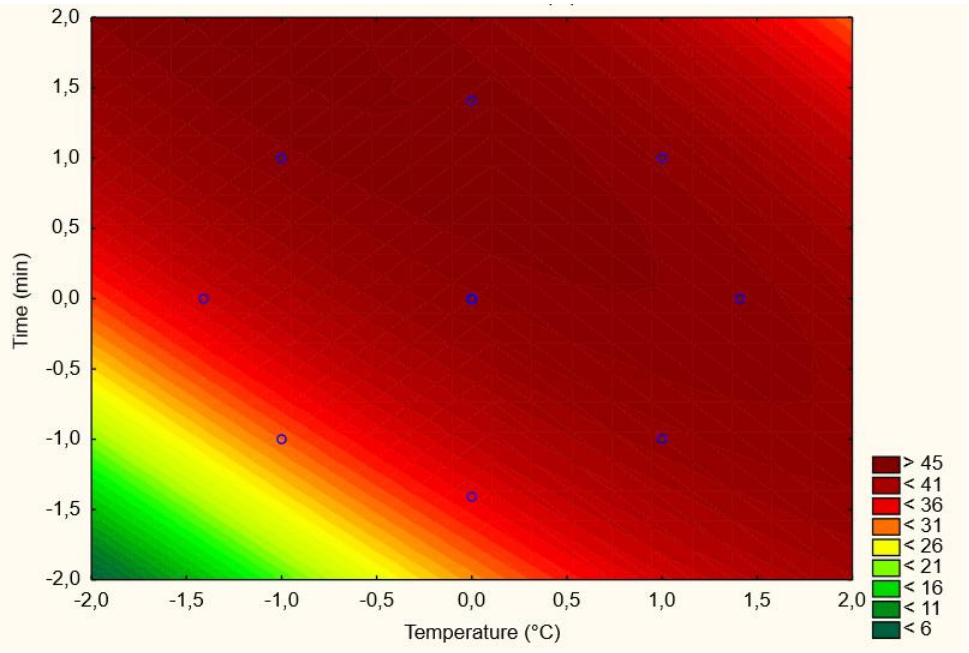

Source: Prepared by the authors.

3.5 Characterization of Co-products

3.5.1 Higher Heating Value

REMUNOM
ISSN 2178-6925

Received: 13/01/2026 - **Accepted:** 02/04/2026
Vol: 13.05
DOI: 10.66104/qfmhys90
Pages: 1-33

The analysis of the Higher Heating Value (HHV) of the obtained materials, bio-oil, and biochar, provides relevant information about their energy potential. The bio-oil, with a mass of 0.3044 g, showed an HHV of 10.68 MJ kg^{-1}, indicating lower energy density. In contrast, the biochar, with a mass of 0.3165 g, presented a significantly higher value of 30.664 MJ kg^{-1}.

This difference is associated with the higher concentration of fixed carbon and the lower presence of oxygenated compounds in biochar, characteristics resulting from the carbonization process. On the other hand, bio-oil presents a high fraction of oxygenated compounds, which contributes to the reduction of its heating value, since these molecules have lower energy density.

The values obtained are consistent with those reported for similar materials, in which biochar presents a higher heating value compared to bio-oil, due to its higher concentration of fixed carbon and lower oxygen content (Liu et al 2019; Wang et al. 2020). In this context, Brózdowski et al. (2025) observed that bio-oil presented a heating value in the range of 18.7 to 22.5 MJ kg^{-1}, reaching approximately 24.1 MJ kg^{-1}. Regarding biochar, studies such as that of Tu et al. (2022) demonstrate that increasing pyrolysis temperature raises the fixed carbon content and, consequently, the heating value of the material. These results corroborate the data obtained in this study, in which biochar exhibited higher energy density compared to bio-oil. Thus, the obtained results indicate that biochar presents a high heating value, a relevant characteristic for energy applications.

These applications demonstrate that, in addition to its high energy performance, biochar stands out as a promising material in the context of renewable and sustainable energy sources (Liu et al 2019).

3.5.2 Fourier Transform Infrared Spectroscopy (FTIR)

FTIR spectra allowed the identification of the main functional groups present in the co-products, whose results are summarized in Figure 9 and Table 7.

REMUNOM
ISSN 2178-6925

Received: 13/01/2026 - **Accepted:** 02/04/2026
Vol: 13.05
DOI: 10.66104/qfmhys90
Pages: 1-33

Figure 9 - Functional groups identified in the FTIR for biochar and bio-oil.

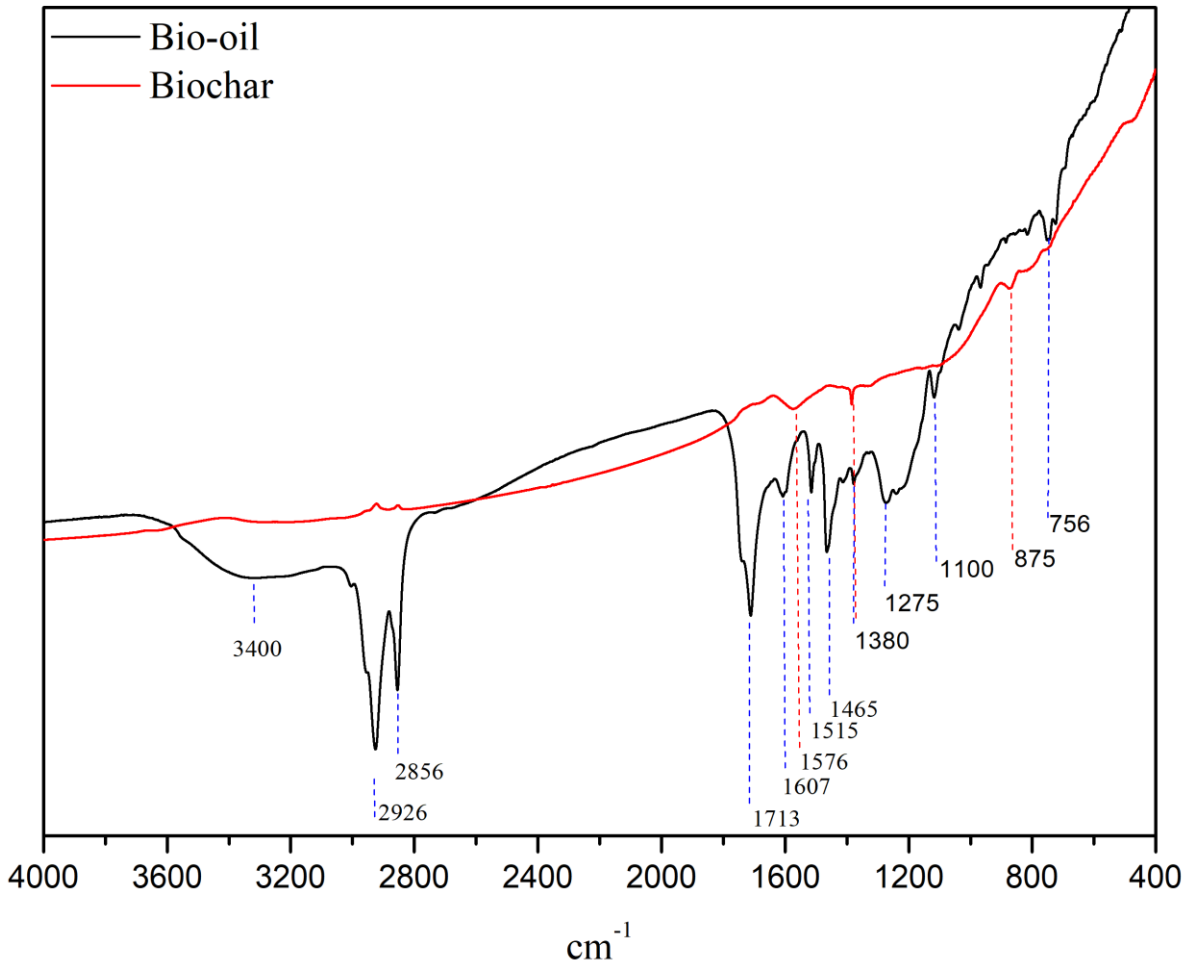

Source: Prepared by the authors.

For bio-oil, a small broad band is observed in the region of 3400 cm^{-1} associated with the stretching vibrations of the –OH bond, typical of hydroxyl groups. This suggests the presence of phenolics, alcohols, carboxylic acids, and water, indicating hydrophilic compounds and moisture, more intensely present in bio-oil. In the regions of 2926 cm^{-1} and 2856 cm^{-1}, the bands represent the asymmetric and symmetric stretching of C–H in alkanes, indicating aliphatic groups in hydrocarbons. The band at 1713 cm^{-1}, is associated with the stretching of the C=O bond, which may indicate the presence of oxygenated compounds, such as carboxylic acids, esters, and ketones, derived from hemicellulose decomposition. The regions of 1607 cm^{-1} and 1515 cm^{-1} represent C=O and C=C vibrations, common in carbonyl groups and alkenes, typical of lignocellulosic structures. The band at 1275 cm^{-1}, associated with

REMUNOM
ISSN 2178-6925

Received: 13/01/2026 - **Accepted:** 02/04/2026
Vol: 13.05
DOI: 10.66104/qfmhys90
Pages: 1-33

C–O stretching, is typical of ethers and phenols, derived from lignin and hemicellulose. The bands around 1100 cm^{-1} reflect the presence of C–O–C and –CH_2 bonds, characteristic of structures derived from cellulose and hemicellulose, reflecting the decomposition process of these fractions.

For biochar there is a band at 1576 cm^{-1}, indicating the presence of C=C bonds derived from lignin that reflect the formation of a carbonaceous structure, referring to aromatic groups.

The bands at 1465 cm^{-1} (bio-oil) and 1380 cm^{-1} (biochar and bio-oil) are associated with the deformation of CH_2, CH_3 and OH bonds, indicating the presence of methyl groups derived from aliphatic or aromatic organic compounds, characteristic of lignocellulosic materials. These bands are more intense in bio-oil, reinforcing the presence of aromatic compounds. Finally, the bands at 875 cm^{-1} (bio-oil) and 756 cm^{-1} (biochar) indicate, respectively, the presence of β-glycosidic linkages, characteristic of polysaccharides such as cellulose, and out-of-plane C–H vibrations in aromatic rings.

The results obtained in this study are similar to those reported for bio-oil and biochar of lignocellulosic origin. The presence of bands associated with hydroxyl groups (~3400 cm^{-1}), aliphatic C–H bonds (2926–2856 cm^{-1}) and carbonyl groups (~1713 cm^{-1}) in bio-oil has also been reported by Mafra et al. (2024) and Salim et al. (2021), indicating the predominance of oxygenated compounds in this fraction. Additionally, the higher intensity of bands associated with C–O–C bonds (~1100 cm^{-1}) in bio-oil, also observed by Sousa et al. (2024), reinforces the higher concentration of oxygenated compounds in the liquid phase.

On the other hand, the presence of bands related to aromatic structures in the region of 1576 cm^{-1} and at ~875 cm^{-1} is consistent with the results described by Janu et al. (2021) and Guo et al. (2022), evidencing the higher degree of aromaticity and structural condensation of biochar.

REMUNOM
ISSN 2178-6925

Received: 13/01/2026 - **Accepted:** 02/04/2026
Vol: 13.05
DOI: 10.66104/qfmhys90
Pages: 1-33

Table 7. Functional groups identified by FTIR.

Wavenumber (cm^{-1})	Functional Group	Biochar	Bio-oil	References
~3400	–OH	Absent	Present (broad)	(Mafra et al 2024; Salim et al 2021)
2926 - 2856	C–H (alkanes, asymmetric stretching)	Absent	Strong	(Silva et al 2023; Mafra et al 2024)
1713	C=O	Absent	Strong	(Mafra et al 2024; Salim et al 2021)
1607, 1576, 1515	C=C (aromatic rings)	Present	Present	(Silva et al 2023; Janu et al 2021; Guo et al. 2022)
1465	CH_2, CH_3	Absent	Strong	(Mafra et al 2024)
1380	CH_2, CH_3, OH	Weak	Weak	(Silva et al 2023)
1275	C–O (esters and phenols)	Absent	Present	(Silva et al 2023)
~1100	C–O–C	Absent	Present (strong)	(Sousa et al. 2024)
875	C–H (out-of-plane vibration in aromatic rings)	Present	Absent	(Sousa et al. 2024)
756	C–H (out-of-plane vibration in aromatic rings)	Absent	Present	(Sousa et al. 2024)

Source: Prepared by the authors.

4. Conclusion

The experimental analysis demonstrates that the distribution of products from the pyrolysis of buriti residue is strongly dependent on the evaluated operational conditions, temperature, and pyrolysis time. It was observed that biochar yield is favored at lower temperatures (30.75% at 450 °C for 30 minutes), while bio-oil production is maximized under intermediate temperature conditions and longer residence times (48.98% at 525 °C for 60 minutes). The statistical analysis using ANOVA indicated that temperature is the most relevant factor for biochar yield, presenting a predominantly linear effect, while time did not show significant influence within the studied range. For bio-oil, on the other hand, both temperature and time exerted significant influence, with emphasis on pyrolysis time as the variable with the greatest impact. It is noteworthy that these results represent more favorable conditions within the evaluated experimental range and do not constitute a global

REMUNOM
ISSN 2178-6925

Received: 13/01/2026 - **Accepted:** 02/04/2026
Vol: 13.05
DOI: 10.66104/qfmhys90
Pages: 1-33

optimization of the process. Additionally, the characterization of the co-products showed that biochar presents a high heating value (30.664 MJ kg^{-1}), while bio-oil (HHV 10.68 MJ kg^{-1}) has a composition rich in oxygenated compounds, as evidenced by FTIR analysis. Finally, the results obtained provide insights into the influence of operational variables on the pyrolysis of buriti residue. As a future perspective, it is recommended to expand the experimental range, especially with respect to residence time, as well as to include additional variables, such as heating rate and particle size, aiming at improving the statistical model and validating the identified conditions, followed by further characterization of the co-products regarding their potential fuel application.

Acknowledgments

This study was funded in part by the Coordenação de Aperfeiçoamento de Pessoal de Nível Superior – Brazil (CAPES) – Financial Code 001.

5. References

ABOELELA, D. *et al.* Recent advances in biomass pyrolysis processes for bioenergy production: optimization of operating conditions. *Sustainability*, v. 15, n. 14, p. 11238, 2023.

AMENAGHAWON, A. N.; ANYALEWECHI, C. L.; OKIEIMEN, C. O. Biomass pyrolysis technologies for value-added products: a state-of-the-art review. *Environmental Engineering Research*, 2021.

BRÓZDOWSKI, J. *et al.* Valorization of forest biomass through pyrolysis: a study on the energy potential of wood tars. *Energies*, v. 18, n. 5, p. 1113, 2025.

CONSUMI, M. *et al.* Analytical composition of flours through thermogravimetric and rheological combined methods. *Thermochemical Acta*, v. 711, p. 179204, 2022.

EMIOLA-SADIQ, T.; ZHANG, L.; DALAI, A. K. Thermal, and kinetic studies on biomass degradation via thermogravimetric analysis: a combination of model-fitting and model-free approach. *ACS Omega*, v. 6, n. 34, p. 22233–22247, 2021.

FERREIRA, Charles Samuel Moraes *et al.* Torta de buriti (Mauritia flexuosa) como ingrediente alternativo em rações para juvenis de Tambaqui (Colossoma

REMUNOM
ISSN 2178-6925

Received: 13/01/2026 - **Accepted:** 02/04/2026
Vol: 13.05
DOI: 10.66104/qfmhys90
Pages: 1-33

macropomum). Research, Society and Development, v. 10, n. 8, p. e24510817345, 11 jul. 2021.

GÓMEZ-SANABRIA, A. *et al.* Potential for future reductions of global GHG and air pollutants from circular waste management systems. *Nature Communications*, v. 13, p. 106, 2022.

GUIMARÃES, Munique Gonçalves *et al.* Green energy technology from buriti (Mauritia flexuosa L. f.) for Brazilian agro-extractive communities. SN Applied Sciences, v. 3, n. 3, p. 283, 6 mar. 2021.

GUO, W. *et al.* Comparison of 17β-estradiol adsorption on corn straw- and dewatered sludge-biochar in aqueous solutions. *Molecules*, v. 27, n. 8, p. 2567, 2022.

JANU, R. *et al.* Biochar surface functional groups as affected by biomass feedstock, biochar composition, and pyrolysis temperature. *Carbon Resources Conversion*, v. 4, p. 36–46, 2021.

JERZAK, W.; ACHA, E.; LI, B. Comprehensive review of biomass pyrolysis: technologies, product distribution, and mechanisms. *Energies*, v. 17, 2024.

LIU, W.-J.; JIANG, H.; YU, H.-Q. Emerging applications of biochar-based materials for energy storage and conversion. *Energy & Environmental Science*, v. 12, n. 6, p. 1751–1779, 2019.

MAFRA, E. R. M. L. *et al.* Comparative analysis of seed biomass from Amazonian fruits for activated carbon production. *Biomass Conversion and Biorefinery*, v. 14, n. 10, p. 11279–11293, 2024.

MYERS, R. H.; MONTGOMERY, D. C.; ANDERSON-COOK, C. M. *Response surface methodology: process and product optimization using designed experiments*. 4. ed. New York: John Wiley & Sons, 2016.

RACERO-GALARAGA, D. *et al.* Proximate analysis in biomass: standards, applications, and key characteristics. *Results in Chemistry*, v. 12, p. 101886, 2024.

SALDARRIAGA, J. F. *et al.* Fast characterization of biomass fuels by thermogravimetric analysis (TGA). *Fuel*, v. 140, p. 744–751, 2015.

SALIM, R.; ASIK, J.; SARJADI, M. S. Chemical functional groups of extractives, cellulose and lignin extracted from native *Leucaena leucocephala* bark. *Wood Science and Technology*, v. 55, n. 2, p. 295–313, 2021.

REMUNOM
ISSN 2178-6925

Received: 13/01/2026 - **Accepted:** 02/04/2026
Vol: 13.05
DOI: 10.66104/qfmhys90
Pages: 1-33

SILVA, J. B. S. da *et al.* Buriti (*Mauritia flexuosa* L.) wastes as potential lignocellulosic feedstock for bioenergy production: physicochemical properties, thermal behavior, and emission factors. *Industrial Crops and Products*, v. 206, p. 117689, 2023.

SOUSA, W. C. de; MORAIS, R. A.; ZUNIGA, A. G. D. Buriti (*Mauritia flexuosa*) shell flour: nutritional composition, chemical profile, and antioxidant potential as a strategy for valuing waste from native Brazilian fruits. *Food Research International*, v. 190, p. 114578, 2024.

TU, P. *et al.* Influence of pyrolysis temperature on the physicochemical properties of biochars obtained from herbaceous and woody plants. *Bioresources and Bioprocessing*, v. 9, n. 131, 2022.

WANG, G. *et al.* A review of recent advances in biomass pyrolysis. *Energy & Fuels*, v. 34, n. 12, p. 15557–15578, 2020.

WANG, W. *et al.* Current challenges, and perspectives for the catalytic pyrolysis of lignocellulosic biomass to high-value products. *Catalysts*, v. 12, n. 12, p. 1524, 2022.

APPENDIX

Figure A. Predicted values vs. residual values for biochar yield.

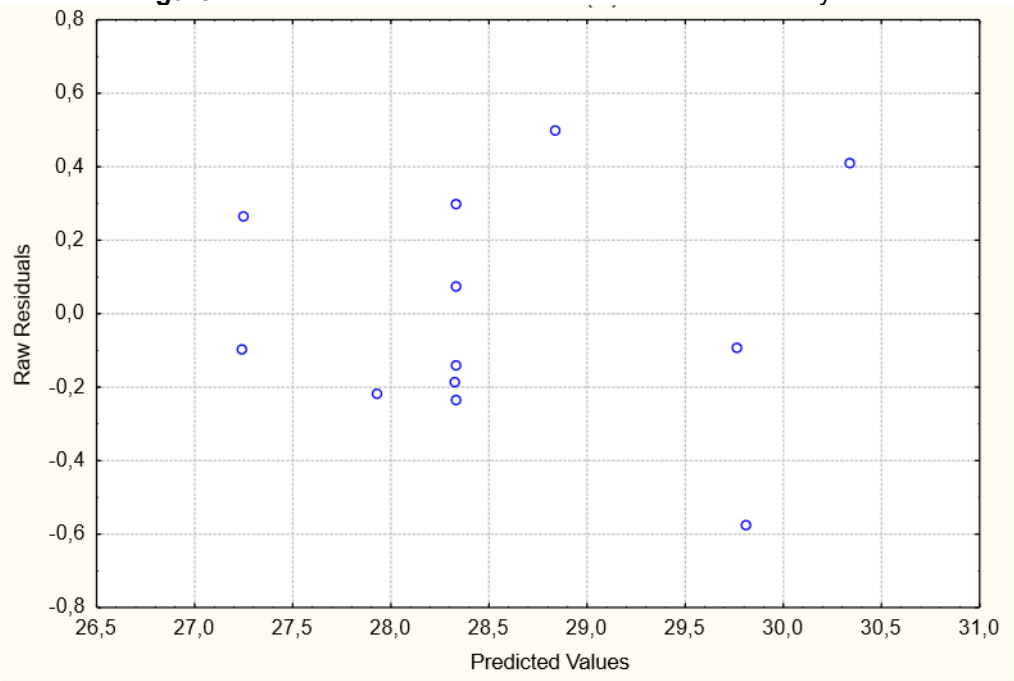

REMUNOM
ISSN 2178-6925

Received: 13/01/2026 - **Accepted:** 02/04/2026
Vol: 13.05
DOI: 10.66104/qfmhys90
Pages: 1-33

Source: Prepared by the authors.

Figure B. Predicted values vs. residual values for bio-oil yield.

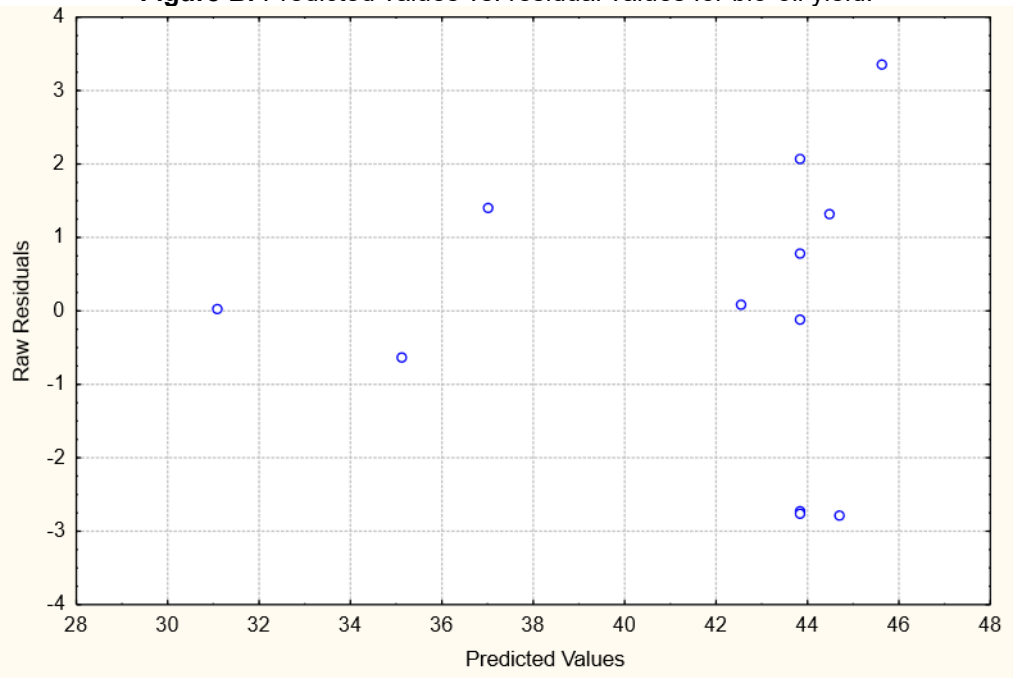

Source: Prepared by the authors.

Figure C. Observed values vs. predicted values for biochar yield.

REMUNOM
ISSN 2178-6925

Received: 13/01/2026 - **Accepted:** 02/04/2026
Vol: 13.05
DOI: 10.66104/qfmhys90
Pages: 1-33

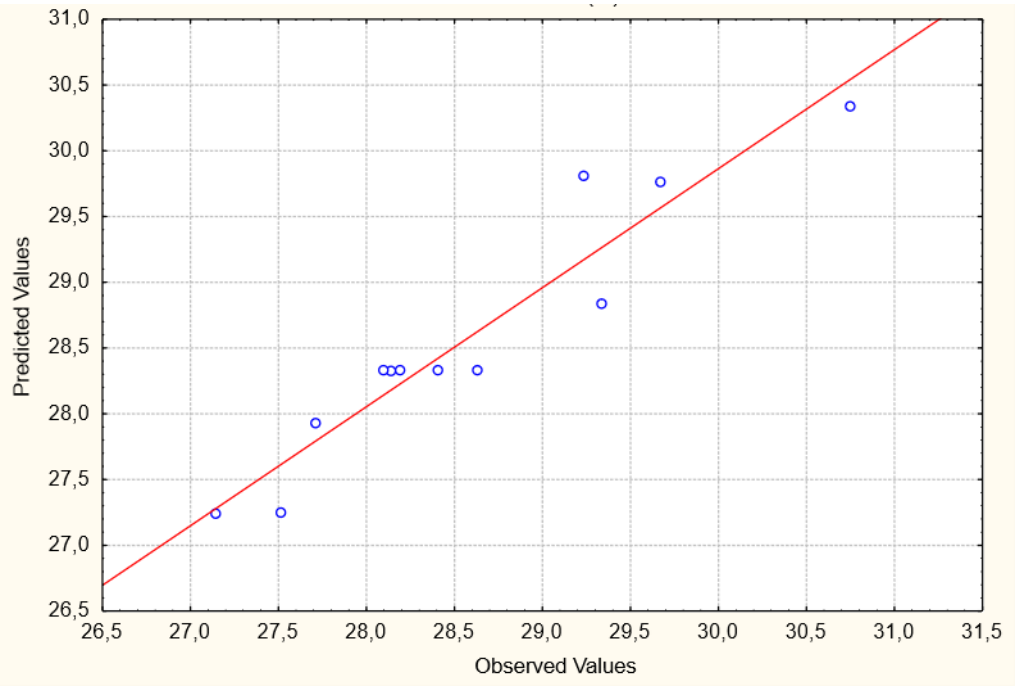

Source: Prepared by the authors.

Figure D. Observed values vs. predicted values for bio-oil yield.

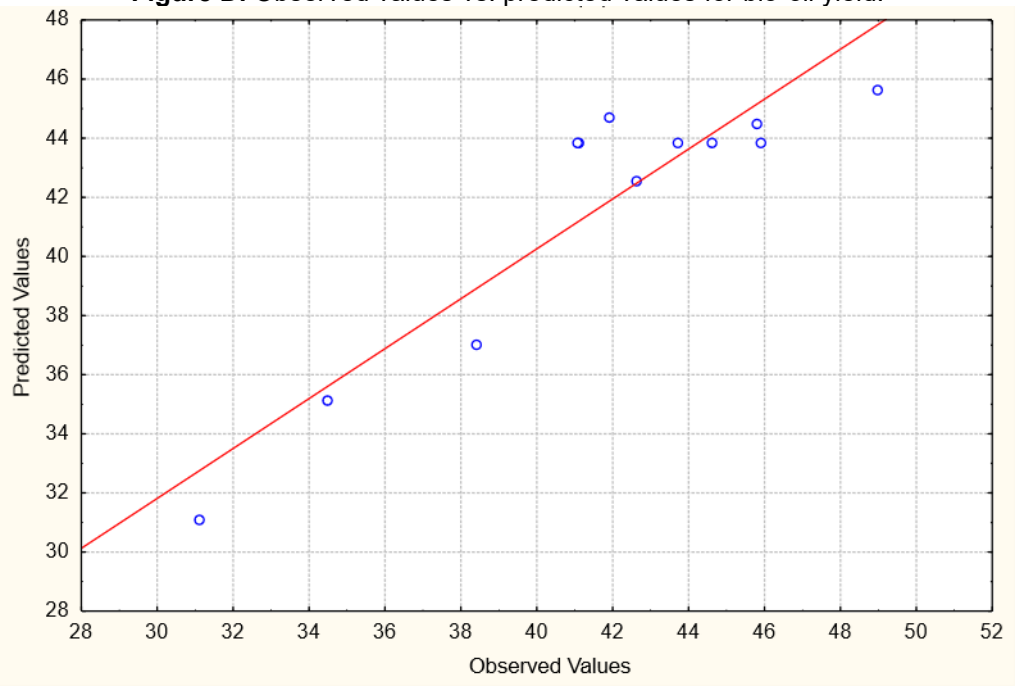

Source: Prepared by the authors.